Title: Identification and quantification of carbamate pesticides in dried lime tree flowers by means of excitation-emission molecular fluorescence and parallel factor analysis when quenching effect exists

Author: L. Rubio M.C. Ortiz L.A. Sarabia

PII: S0003-2670(14)00191-3
DOI: http://dx.doi.org/doi:10.1016/j.aca.2014.02.008
Reference: ACA 233101

To appear in: *Analytica Chimica Acta*

Received date: 14-11-2013
Revised date: 31-1-2014
Accepted date: 6-2-2014

Please cite this article as: L.Rubio, M.C.Ortiz, L.A.Sarabia, Identification and quantification of carbamate pesticides in dried lime tree flowers by means of excitation-emission molecular fluorescence and parallel factor analysis when quenching effect exists, Analytica Chimica Acta http://dx.doi.org/10.1016/j.aca.2014.02.008

IDENTIFICATION AND QUANTIFICATION OF CARBAMATE PESTICIDES IN DRIED LIME TREE FLOWERS BY MEANS OF EXCITATION-EMISSION MOLECULAR FLUORESCENCE AND PARALLEL FACTOR ANALYSIS WHEN QUENCHING EFFECT EXISTS

L. Rubio [a], M.C. Ortiz [a,*], L.A. Sarabia [b]

[a] *Department of Chemistry,* [b] *Department of Mathematics and Computation*

Faculty of Sciences, University of Burgos

Plaza Misael Bañuelos s/n, 09001 Burgos (Spain)

* Corresponding author. Telephone number: 34-947-259571. E-mail address: mcortiz@ubu.es (M.C. Ortiz).

HighlightsHIGHLIGHTS ► Determination of carbamate pesticides in dried lime tree flowers by EEM and PARAFAC ► Quenching effect and overlapping spectra are solved by three way techniques ► The second order property of PARAFAC decomposition is useful to solve problems in EEM ► Using PARAFAC to select the adequate dilution that minimizes the quenching effect ► A procedure to choose a D-optimal design for a multi-analyte standard addition method

Abstract

A non-separative, fast and inexpensive spectrofluorimetric method based on the second order calibration of excitation-emission fluorescence matrices (EEMs) was proposed for the determination of carbaryl, carbendazim and 1-naphthol in dried lime tree flowers. The trilinearity property of three-way data was used to handle the intrinsic fluorescence of lime flowers and the difference in the fluorescence intensity of each analyte. It also made possible to identify unequivocally each analyte. Trilinearity of the data tensor guarantees the uniqueness of the solution obtained through parallel factor analysis (PARAFAC), so the factors of the decomposition match up with the analytes. In addition, an experimental procedure was proposed to identify, with three-way data, the quenching effect produced by

the fluorophores of the lime flowers. This procedure also enabled the selection of the adequate dilution of the lime flowers extract to minimize the quenching effect so the three analytes can be quantified. Finally, the analytes were determined using the standard addition method for a calibration whose standards were chosen with a D-optimal design.

The three analytes were unequivocally identified by the correlation between the pure spectra and the PARAFAC excitation and emission spectral loadings. The trueness was established by the accuracy line “calculated concentration *versus* added concentration” in all cases. Better decision limit values (CCα), in $x_0 = 0$ with the probability of false positive fixed at 0.05, were obtained for the calibration performed in pure solvent: 2.97 μg L^{-1} for 1-naphthol, 3.74 μg L^{-1} for carbaryl and 23.25 μg L^{-1} for carbendazim. The CCα values for the second calibration carried out in matrix were 1.61, 4.34 and 51.75 μg L^{-1} respectively; while the values obtained considering only the pure samples as calibration set were: 2.65, 8.61 and 28.7 μg L^{-1}, respectively.

Abbreviations

Excitation-emission fluorescence matrix (EEM), parallel factor analysis (PARAFAC), decision limit (CCα), unfolded partial least-squares with residual bilinearization (U-PLS/RBL), polycyclic aromatic hydrocarbons (PAHs), self-weighted alternating trilinear decomposition (SWATLD), alternating penalty trilinear decomposition (APTLD), multivariate curve resolution-alternating least squares (MCR-ALS), maximum residue limit (MRL), high-performance liquid chromatography (HPLC), diode array detection (DAD), liquid chromatography with mass spectrometry detection (LC/MS), liquid chromatography coupled to tandem mass spectrometry (LC/MS-MS), Rapid Alert System for Food and Feed (RASFF), central composite design (CCD), core consistency diagnostic (CORCONDIA), International Organization for Standardization (ISO), International Union of Pure and Applied Chemistry (IUPAC), capability of detection (CCβ), least squares (LS).

Keywords: excitation-emission fluorescence; Parallel Factor Analysis; carbamate pesticides; quenching effect; capability of detection; dried lime tree flowers

1. Introduction

The most habitual methods of analysis usually include time-consuming procedures, for example, extraction and/or preconcentration followed by chromatographic separation processes [1]. Nowadays, owing to the increase in the number of samples to control, it is important to provide simple and inexpensive methods for the determination of toxic residues and pollutants in fields under legislation.

In this sense, fluorescence spectroscopy presents a high potential owing to its high sensitivity, ease of use and availability of portable instruments. In addition, molecular fluorescence measurements can be carried out quickly and at low cost. However, because spectroscopy covers a wide range of excitation and emission wavelengths, the signals of the analytes of interest may be overlapped with each other, with the fluorescent matrix constituents in complex mixtures and even present quenching effect. This makes the determinations difficult to a great extent, decreases the selectivity of the method and requires the use of separation techniques prior to the use of spectrofluorimetric techniques to obtain a specific univariate signal. An alternative is the use of excitation-emission fluorescence matrices (EEMs) coupled with chemometric methods that exhibit the second-order property. Thus, the identification and quantification of the analytes of interest are possible even in the presence of non-calibrated interferences [2]. Several chemometric methods with the second-order property have been applied to EEM matrices to solve these difficulties.

By way of example, Alarcón et al. [3] have used the unfolded partial least-squares with residual bilinearization (U-PLS/RBL) algorithm to resolve a mixture of heavy polycyclic aromatic hydrocarbons (PAHs) in edible oils, in the presence of other PAHs not included in the analysis. However, the presence of compounds that produce inner filter effect required the sample pretreatment for the determination of these PAHs.

Using EEM and the self-weighted alternating trilinear decomposition (SWATLD) algorithm, Qing et al. [4] have determined 2-naphthoxyacetic acid and 1-naphthaleneacetic acid methyl ester in soil samples and in sewage samples with quenching effect.

In reference [5] the alternating penalty trilinear decomposition (APTLD) algorithm is proposed to determine napronamide in environmental samples through EEMs and to handle the fluorescent interferences as well as the overlapping of the fluorescent signal between the analyte and the background of the samples.

The multivariate curve resolution-alternating least squares (MCR-ALS) method has been used together with excitation-emission fluorescence data and UV-Vis spectroscopy in Ref. [6] to analyze the interactions of mixtures of two β-agonists steroids with bovine serum albumin with overlapping spectral profiles.

The application of Parallel Factor Analysis (PARAFAC) to EEM data has satisfactorily resolved the overlapping signals of the analytes in complex matrices, such as, milk [7], whey [8], urine [9,10,11], cosmetics [12] and human plasma [13]. Ortiz et al. [**Error! Bookmark not defined.**] identified and quantified ciprofloxacin in urine samples through second-order fluorescent signals and three-way PARAFAC calibration. They also carried out the study in the presence of another analyte (mesalazine) fluorescent in the same region as the analyte of interest. Moreover, the spectra of the urine and the mesalazine are overlapped with the one of the ciprofloxacin. In references [**Error! Bookmark not defined.**,**Error! Bookmark not defined.**,**Error! Bookmark not defined.**], PARAFAC was applied in the standard addition mode. Theoretically, the physical model of the quenching effect is a quadrilinear model [14] and it has been used in the determination of tetracycline under the strong quenching effect made by tea [15]. The ability of PARAFAC to resolve highly overlapped spectral profiles in the trace determination of carbamate pesticides, in solvent matrix, has also been shown in Ref. [16].

The use of pesticides for years has led to a significant reduction in crop losses due to insects, weeds and plant diseases contributing to satisfy the growing demand of agricultural products worldwide. However, the toxicological properties of these pesticides pose a risk to

the environment and human health [17]. For this reason, several national and international organizations have established maximum residue limits (MRL) in food treated with them to protect the health of consumers. These MRLs are specific to combinations of pesticides and food commodities. Carbamate pesticides, which are derivatives of carbamic acid, are widely used but they have toxic effects. They present many applications (fungicides, herbicides …) and are commonly used as insecticides due to their neurotoxic effect as inhibitors of the enzyme acetylcholinesterase [18], which is responsible for the transmission of nervous impulses.

The determination of carbamates can be carried out using several techniques, such as high-performance liquid chromatography (HPLC) with fluorescence detection [19], with diode array detection (DAD) [20], or with UV detection [21]; liquid chromatography with mass spectrometry detection (LC/MS) [22] or with tandem mass spectrometry detection (LC/MS-MS) [23,24]. Thermal instability and polarity of many carbamates have limited the use of gas chromatography for their determination [25]. This limitation can be eliminated using a previous derivatization step, which involves an increase of the analysis time and less precision in the procedures used. The aforementioned methods usually have certain disadvantages such as extraction, cleanup and concentration steps of the extract are required, which are time-consuming, and that instrumentation is expensive.

Several works that use EEM for the determination of carbamate pesticide residues can be found in the literature [**Error! Bookmark not defined.**, 26,27,28]. Due to carbamates exhibit native fluorescence, carbaryl and its degradation product 1-naphthol are determined in water in [**Error! Bookmark not defined.**]. The concentrations of both analytes were determined through the hydrolysis kinetics of carbaryl to 1-naphthol adjusted with the loadings of a PARAFAC decomposition. Previously, the authors have shown the absence of interferences in the fluorescent signals recorded.

The aim of this work is to generalize the use of EEM spectra to determine carbamate pesticides in matrices that produce interferences and quenching effect but avoiding the use of four-way tensors that require a broad experimentation because in this case it is necessary

to modify the quantity of quencher and then to generate for each level of the quencher a complete three-way tensor formed by as many EEM matrices as calibration samples. Specifically, the determination of two carbamate pesticides (carbaryl and carbendazim) and of the degradation product of carbaryl (1-naphthol) was carried out with EEM data and PARAFAC. The chemical structures of these compounds are shown in Fig. 1. This analysis was performed on samples prepared in methanol to provide the reference spectra as well as the figures of merit of the calibration based on a PARAFAC decomposition. To carry out the analysis in dried lime tree flowers, an extraction with ethyl acetate was performed without further purification.

Lime flowers have fluorophores with fluorogenic activity in the same spectral region as the analytes and also present a strong quenching effect. Therefore, in a second stage, this effect was analyzed through the loadings of a PARAFAC decomposition. As a result, the appropriate dilution of the sample that allows a reproducible calibration was obtained. The concentrations of the mixtures were distributed using a D-optimal experimental design and the figures of merit in the determination of carbamates in dried lime tree flowers were obtained.

The maximum residue limit (MRL) for carbaryl and carbendazim in herbal infusions such as lime flowers has been set at 100 μg Kg^{-1} as it is established in Commission Regulation (EC) No. 149/2008 [29] and Commission Regulation (EU) No. 559/2011 [30], respectively. Even so, it is necessary to note that Commission Regulation (EC) No. 899/2012 [31] establishes that the MRL for carbaryl "*shall be reviewed in 1 year, to evaluate monitoring data on the occurrence of carbaryl in herbal infusions*"; therefore this value is susceptible of change in the near future.

However, the need to monitor the levels of pesticide residues in food commodities and the increase in the number of samples to control, caused by the increase in trade relations, require sensitive, cheap and fast analytical methods. Some details of the current status of this issue in relation to carbendazim and carbaryl are shown below. The Rapid Alert System for Food and Feed (RASFF) [32] of the European Commission has reported 138 notifications

for carbendazim from 23/08/2001 to 25/07/2013 distributed as follows: 7 alert notifications, 55 border rejection notifications, 51 information notifications, 23 information for attention notifications and 2 information for follow-up notifications. Some amounts found in fruits, vegetables, herbs and spices were: 10 mg kg^{-1} in chilled mint, 7.38 mg kg^{-1} in fresh okra, 4.8 mg kg^{-1} in aubergines, 1.5 mg kg^{-1} in chamomile blossoms, 26 mg kg^{-1} in broccoli, 12 mg kg^{-1} in papaya, 14.8 mg kg^{-1} in celery leaves, 6.7 mg kg^{-1} in fresh red grapes and 6.6 mg kg^{-1} in green beans. These values are possibly due to the long persistence of carbendazim, which decomposes in the environment with half-lives of 6 to 12 months on bare soil, 3 to 6 months on turf, and half-lives in water of 2 and 25 months under aerobic and anaerobic conditions, respectively [33].

From 29/09/2005 to 16/07/2013, a total of 27 notifications for carbaryl were transmitted through the RASFF: 3 alert notifications, 4 border rejection notifications, 12 information notifications and 8 information for attention notifications. It is calculated the approximate biological half-life of carbaryl in wheat treated to be 40 weeks at 35°C, 60 weeks at 30°C, 80 weeks at 25°C and much longer than 80 weeks at 20°C. Under aerobic conditions, the compound degrades rapidly by microbial metabolism with half-lives of 4 to 5 days in both soil and aquatic environments. In anaerobic environments metabolism is much slower, with half-lives on the order of 2 to 3 months [**Error! Bookmark not defined.**]. The registered concentrations for carbaryl in the RASFF notifications are lower than for carbendazim due to its lower persistence: 1.9 mg kg^{-1} in apricots, 13 mg kg^{-1} in vine leaves, 2.2 mg kg^{-1} in celery, 1.4 mg kg^{-1} in red wine and 7 mg kg^{-1} in fresh apricots. Therefore, the high use of carbendazim and carbaryl in agrarian activity along with their persistence resulted in the need to control them by sensitive, cheap and fast analytical methods as the one proposed in this work for their determination in vegetal, fruits, herbs and spices.

2. Material and methods

2.1. Reagents and standard solutions

Carbaryl (CAS no. 63-25-2) and carbendazim (CAS no. 10605-21-7) (PESTANAL® grade, analytical standard) were obtained from Sigma-Aldrich (Steinheim, Germany). 1-naphthol (CAS no. 90-15-3), methanol (CAS no. 67-56-1) (for liquid chromatography LiChrosolv®) and ethyl acetate (CAS no. 141-78-6) (for gas chromatography SupraSolv®) were purchased from Merck KGaA (Darmstadt, Germany).

Stock solutions of carbaryl, carbendazim and 1-naphthol were prepared individually in methanol at a concentration of 400 mg L^{-1} and stored at low temperature (4ºC). Afterwards, solutions of carbaryl (5 mg L^{-1}), carbendazim (5 mg L^{-1}) and 1-naphthol (2 mg L^{-1}) were prepared in methanol from the stock solutions.

Commercial samples of dried lime tree flowers were analyzed in this work.

2.2. Instrumental

A ZX^3 vortex mixer was purchased from VELP Scientifica (Usmate (MB), Italy). The glass microfiber filters, GF/C grade, 1.2 µm Whatman™ were supplied by GE Healthcare (Little Chalfont, UK). The evaporation of the solvent was performed using a miVac Modular Concentrator (GeneVac Limited, Ipswich, UK) which consisted of a miVac Duo concentrator, a SpeedTrap™ (condenser) and a Quattro pump.

The excitation-emission fluorescence measurements were performed at room temperature on a PerkinElmer LS 50B Luminescence Spectrometer equipped with a xenon discharge lamp. A 10 mm quartz cell with cell volume of 3.5 mL (SUPRASIL®) was used in the analysis. The emission spectra were recorded between 295 nm and 500 nm (each nanometer) at excitation wavelengths between 240 nm and 290 nm (regular steps of 5 nm). Excitation and emission monochromator slit-widths were both set to 10 nm. The scan speed was 1500 nm min^{-1}.

2.3. Experimental procedure

The contents of a commercial lime flower tea bag were placed in a beaker and 10 mL of ethyl acetate was added. Then, the mixture was manually stirred for 30 s and it was stirred for another 30 s using a vortex mixer. The extract was filtered and 6 mL was transferred into

a conical glass tube. The evaporation of the extract to dryness was performed at 40 ºC using a miVac Modular Concentrator. Once the extract was evaporated, it was reconstituted with 6 mL of methanol. The final extract was filtered again to remove solid particles.

To perform the standard addition method, this procedure was repeated for several lime flower tea bags. The resulting filtrates were collected in an amber bottle to obtain a single extract and eliminate the variability. These extracts were stored under refrigeration at 4 ºC. The D-optimal design samples were prepared as follows: 1 mL of the dried lime tree flowers extract and the appropriate volume of the solutions of each of the analytes were added into 5 mL volumetric flasks and completed to the mark with methanol for each experiment.

2.4. Software

Both central composite (CCD) and D-optimal experimental designs were built with NEMRODW [34]. The FL WinLab software (PerkinElmer) was used to register the fluorescent signals through excitation-emission matrices. The data were imported to Matlab using the INCA software [35] that inserts missing values (not-a-number: NaN) into the matrix in the wavelengths that correspond to the Rayleigh effect. PARAFAC models were performed with the PLS_Toolbox 6.0.1 [36] for use with Matlab version 7.12.0.635 (R2011a) (The MathWorks). The linear regressions were built and validated with the statistical program STATGRAPHICS [37]. The figures of merit (CCα and CCβ) were calculated with DETARCHI [38] and CCα and CCβ at the maximum residue limit were estimated using NWAYDET (a home-made program that evaluates the probabilities of false non-compliance and false compliance for n-way data).

3. Theory

3.1. PARAFAC decomposition

For the case of three-way data, PARAFAC (Parallel Factor Analysis) decomposes the original data tensor, **X** (of dimension $I \times J \times K$), into triads or components [39,40]. Each

component consists of three loading vectors. The trilinear PARAFAC model, when the fluorescence intensities are arranged as a three-way tensor **X**, is:

$$x_{ijk} = \sum_{f=1}^{F} a_{if} b_{jf} c_{kf} + \propto_{ijk}, i = 1,..., I, j = 1,..., J, k = 1,..., K \quad (1)$$

where F is the number of factors (fluorophores), a_{if} , b_{jf} and c_{kf} are the elements of the three loading vectors for each factor (f =1,…, F): sample mode, a_f , emission mode, $\mathbf{b}_f$, and excitation mode , $\mathbf{c}_f$. Finally, ε_{ijk} is the residue that is not explained by the trilinear model. The matrices **A** (dimension I × F), **B** (dimension J × F) and **C** (dimension K × F) hold the PARAFAC loading vectors.

When a tensor of experimental data is compatible with the structure in Eq. (1) it is said that the data are trilinear and the estimation by least squares of all the coefficients that intervene in the cited equation is unique [41]. This is the second-order advantage in chemical analysis [42].

A sufficient condition that must be fulfilled by an experimental data set in order for it to be compatible with a trilinear model is that the factors should be the same in all samples, differing only in their sizes. This guarantees the uniqueness of the solution [**Error! Bookmark not defined.**] and, as a result, the unequivocal identification of analytes by means of its emission and excitation spectra.

When *F* fluorophores are contained in *I* samples at the same quantities, the tensor has a unique matrix for all its slabs. The model that describes these data would have the following structure $\mathbf{B}_{JF}\mathbf{D}_{FF}\left(\mathbf{C}^t\right)_{FK}$, where the matrices **B** and **C** contain the *F* emission and excitation spectra of the fluorophores and **D** is the diagonal formed by proportional values to the quantities of the *F* fluorophores. The decomposition of the tensor formed by these *I* matrices is not unique because if **Q** is any orthogonal matrix of dimension (F × F) a new decomposition is generated $\mathbf{B}_{JF}\mathbf{D}_{FF}\left(\mathbf{C}^t\right)_{FK} = \left(\mathbf{B}_{JF}\mathbf{D}_{FF}^{1/2}\mathbf{Q}_{FF}\right)\mathbf{I}_{FF}\left(\mathbf{C}_{KF}\mathbf{D}_{FF}^{1/2}\mathbf{Q}_{FF}\right)^t$. As a consequence, there are infinite different models that provide the same least squares fit; that

is, the decomposition is not unique and the tensor cannot be trilinear. The structure described above is similar to the background obtained when a standard addition method is used with EEM data.

The most useful application of the second-order advantage is that it is possible to identify and quantify the analyte of interest in the presence of unknown interferents because, in this case, the interferent(s) will appear as new factor(s) without affecting the rest. In Ref. [**Error! Bookmark not defined.**], the similarity between the trilinear PARAFAC model and the physical model for fluorescence and a brief description of the steps to be followed to make a calibration model based on PARAFAC and n-way data are shown. A practical description of how to apply PARAFAC modelling to fluorescence excitation-emission measurements can be consulted in Ref. [**Error! Bookmark not defined.**].

3.2. Core Consistency diagnostic

In theory, the model of equation (1) is valid for describing the structure of the EEM data, but in many cases the matrix containing the analytes has fluorophores that do not fit the PARAFAC model. As a consequence, given a tensor of EEM data, we need to decide the validity of the assumption of trilinearity. The Core Consistency Index, CORCONDIA, has been developed for this purpose in ref. [43]. Its description and some details of its practical use are below.

The PARAFAC model of eq. (1) can be written as a sum of rank-one arrays as:

$$\underline{\mathbf{X}}_{IJK} = \sum_{f=1}^{F} \mathbf{a}_f \otimes \mathbf{b}_f \otimes \mathbf{c}_f + \underline{\mathbf{EP}}_{IJK} \qquad (2)$$

so only *F* terms are needed to reconstruct the data tensor.

Assume that a PARAFAC model has been fitted. The model is given by the parameter matrices **A**, **B**, **C** and each addend in eq. (2) has a coefficient equal to one. The PARAFAC core tensor is the core tensor constructed from matrices **A**, **B** and **C** to see if the PARAFAC loadings vectors alone describe the data almost as well as does the model involving interactions of these vector loadings. For this task, the full Tucker3 model was fitted to the

data tensor, but using the loadings found by PARAFAC, obtaining the optimal tensor **G** (dimension F × F × F) that provides the best approximation by least squares of the experimental data tensor. Therefore, the following decomposition is obtained

$$\underline{\mathbf{X}}_{IJK} = \sum_{p=1}^{F}\sum_{q=1}^{F}\sum_{r=1}^{F} g_{pqr}\ \mathbf{a}_p \otimes \mathbf{b}_q \otimes \mathbf{c}_r + \underline{\mathbf{ET}}_{IJK} \tag{3}$$

where the residual tensor $\mathbf{ET}_{IJK}$ is different from that in eq. (2). Considering the structure of equation (3), it is clear that a PARAFAC model is a special case of Tucker3 model with a (F × F × F) tensor **T** = (t_{pqr}) having ones in the superdiagonal (t_{pqr}=1 if p=q=r) and zeros outside. The Tucker3 core tensor, **G**, can be considered as the regression of the experimental data tensor, **X**, on the subspace spanned by the loadings matrices, **A**, **B** and **C**. Therefore, **G**, is the optimal representation of the data tensor in this subspace whereas the PARAFAC model is a constrained regression in the same subspace, because specifically disregards any variation associated with off-superdiagonal core elements.

A way to asses if **G** and **T** are similar is to quantify the Frobenius distance between them. The CORCONDIA index is this distance written as relative similarity (in percentage) against the norm of **T:**

$$\begin{aligned} CORCONDIA &= 100\left(1 - \frac{\sum_{p=1}^{F}\sum_{q=1}^{F}\sum_{r=1}^{F}\left(g_{pqr} - t_{pqr}\right)^2}{\sum_{p=1}^{F}\sum_{q=1}^{F}\sum_{r=1}^{F}\left(t_{pqr}\right)^2}\right) \\ &= 100\left(1 - \frac{\sum_{\{(p,q,r)\neq(f,f,f)\}}\left(g_{pqr}\right)^2 + \sum_{f=1}^{F}\left(g_{fff} - 1\right)^2}{F}\right) \end{aligned} \tag{4}$$

where the addends of the numerator have been separated into two groups: those who are outside the superdiagonal and those in it.

A CORCONDIA close to 100% implies an appropriate model, because **G** and **T** are similar so the best fit (Tucker3) is similar to PARAFAC one and the dimension-wise trilinear combination of vector loadings are the only entities needed for describing the data tensor

and that interactions between them do not contribute appreciably. There is not a threshold accepted by all practitioners, but the closeness to 100% is to be understood relative to the changes compared with models with fewer components.

All off-superdiagonal terms in eq. (4) are positive. If all of them are null then $\sum_{\{(p,q,r)\neq(f,f,f)\}} \left(g_{pqr}\right)^2 = 0$ and necessarily $g_{fff} = 1, f = 1,...F$. If this is not true, there would be a different PARAFAC model, namely $\sum_{f=1}^{F} g_{fff}\ \mathbf{a}_f \otimes \mathbf{b}_f \otimes \mathbf{c}_f$, with a better least squares fit than the initial PARAFAC model $\sum_{f=1}^{F} \mathbf{a}_f \otimes \mathbf{b}_f \otimes \mathbf{c}_f$. This is impossible because the latter has by construction the smallest residual sum of squares. If CORCONDIA is negative, it is fulfilled that $\sum_{\{(p,q,r)\neq(f,f,f)\}} \left(g_{pqr}\right)^2 + \sum_{f=1}^{F} \left(g_{fff} - 1\right)^2 > F > 0$ and, as a result of the above reasoning, at least one of the off-superdiagonal terms is not null, therefore the tensor is not trilinear.

In ref. [44] Bro (pp. 115-118) also proposed to construct a core consistency plot that has the values of the **G** tensor on the vertical and the core elements themselves on the horizontal axis with the superdiagonal elements plotted first.

It has already been shown in ref. [**Error! Bookmark not defined.**] that the core consistency greatly improves when the data which does not follow a trilinear structure is deleted (e.g. when the Rayleigh scatter or the null fluorescent intensity at emission below the recorded excitation wavelength is removed in an EEM tensor). That is, if an experimental tensor is composed of a tensor with trilinear structure added with another which is not; then, it is possible to recover the trilinearity removing the tensor with non-PARAFAC structure.

4. Results and discussion

4.1. Calibration (based on PARAFAC) in methanol.

To carry out the calibration in methanol, a distribution of concentrations for the three analytes studied in this work was chosen in the form of a central composite design (CCD) including: six replicates, the three pure analytes and three methanol blanks. The three blank replicates were measured throughout the experimentation to assure the absence of instrumental drift. As this CCD design has 15 experiments, there were 27 measurements in total. The centre point of the design and the step of variation of the factors were 50 μg L^{-1} and 25 μg L^{-1} (for carbaryl), 100 μg L^{-1} and 50 μg L^{-1} (for carbendazim) and 20 μg L^{-1} and 10 μg L^{-1} (for 1-naphthol) respectively. The last analyte is more fluorescent than the other two above mentioned. The axial points of the CCD have been placed at distance 2; thus, the concentration range was: 0-100 μg L^{-1} for carbaryl, 0-200 μg L^{-1} for carbendazim and 0-40 μg L^{-1} for 1-naphthol and each analyte was at five levels of concentration. Table S1 of the "Electronic Supplementary Material" shows the concentration of the different calibration samples prepared in methanol.

The tensor **X** (27 × 206 × 11) contains the EEM matrices in the order shown in Table S1. The first mode corresponds to the number of samples (27), whereas 206 and 11 are the number of emission and excitation wavelengths recorded, respectively. The PARAFAC model was built with the non-negativity constraint on the three ways, as both the excitation and emission spectra must always be positive. Four factors were chosen, with a CORCONDIA value equal to 87% and explained variance of 99.93%. No outlier data were found, once Q and Hotelling's T^2 indices were applied. The loadings of the sample, emission and excitation modes for each of the four factors of the PARAFAC model are included in Fig. 2. From the observation of the loadings, it is deduced that three of the factors correspond to the studied analytes (carbaryl, carbendazim and 1-naphthol) and the fourth factor is the background.

The wavelengths, that provided the maximum fluorescence intensity in the recorded region, have been determined from the EEM matrices of the pure analytes (see Fig. 3). For emission, these wavelengths were 309 nm for carbendazim, 334 nm for carbaryl and 356 nm for 1-naphthol and the excitation spectrum was taken in each of them. The maximum

excitation intensities were obtained at 280 nm, 275 nm and 240 nm, respectively. The emission spectrum was considered in each of these wavelengths. Thus, the reference spectra that allow the identification of the analytes by their correlation with the spectral loadings estimated from the PARAFAC model obtained (Fig. 2 (b) and (c)) are available. The correlation coefficients for the emission and excitation profiles were 0.999 and 0.997 for 1-naphthol (first factor); 0.990 and 0.997 for carbaryl (second factor); and 0.985 and 0.974 for carbendazim (third factor), respectively. Therefore, the factors estimated from the PARAFAC model are identified with the analytes.

The analysis of Fig. 3 shows that a high fluorescent overlapping exists between carbaryl and carbendazim; especially in the emission range from 300 nm to 350 nm and in the excitation range from 270 nm to 290 nm. In addition, carbaryl, carbendazim and 1-naphthol are overlapped in the emission range between 295 nm and 420 nm. This is also observed in the mixture solution of the three analytes (see Fig. 3(d)). In Fig. 3, it is also found that the order of the fluorescence intensity of the analytes is: 1-naphthol > carbaryl > carbendazim. The fluorescence intensity of carbendazim is very low compared to the other analytes studied in this work and it is totally overlapped with them, which makes its determination difficult. In fact, it would be impossible its univariate quantification with the maximum fluorescence intensity.

A calibration line of “sample mode loadings v*ersus* true concentration” was fitted and validated for each of the three studied analytes with the calibration samples, that is, all the samples except for the six replicates used as prediction set. Only sample 8 for carbendazim should be considered as outlier (absolute value of standardized residual higher than 2.5) and, thus, it has been removed. The results of the analyses are shown in Table 1. The lowest values of the mean of the absolute values of the relative errors were obtained for carbaryl: 4.13% (n=15) in calibration and 3.48% (n=5) in prediction; whereas the higher values were obtained for carbendazim: 10.07% (n=14) and 10.90% (n=6), respectively. Next, the accuracy lines were performed, that is, the regressions “calculated concentration with the sample loadings obtained from the PARAFAC decomposition *versus* true concentration”. In

all cases, the property of trueness was fulfilled, because the p-values of the hypothesis test for the slope and the intercept were higher than 0.05, and thus, the intercept and the slope were significantly equal to 0 and 1, respectively. The parameters of this regression are collected in Table 1. Furthermore, the precision, as standard deviation of these three regressions, is included.

The International Organization for Standardization (ISO) in its norm ISO 11843 [45] defines the decision limit, CCα, as *"the value of the net concentration the exceeding of which leads, for a given error probability α, to the decision that the concentration of the analyte in the analyzed material is larger than that in the blank material*". Whereas the capability of detection or minimum detectable net concentration, x_d or CCβ, has been defined for a given probability of false positive α, as *"the true net concentration of the analyte in the material to be analyzed which will lead, with probability 1 −β, to the correct conclusion that the concentration in the analyzed material is larger than that in the blank material"*. The need of assessing both the probabilities of false positive, α, and of false negative, β, has also been recognised by the International Union of Pure and Applied Chemistry (IUPAC) [46] and other European regulations [47]. The generalization of the procedure to obtain the decision limit (CCα) and the capability of detection (CCβ) with multivariate and/or multiway calibrations can be found in Ref. [48].

The lowest values of CCα and CCβ (for α = β = 0.05) in x_0 = 0 were obtained for 1-naphthol, with values of 2.97 μg L^{-1} and 5.86 μg L^{-1} respectively, while the values for carbendazim were 23.25 μg L^{-1} and 45.89 μg L^{-1}, respectively. These values for carbendazim were higher than for the rest due to two facts: the heavy overlapping of its fluorescence signal with the other analytes in the chosen region and its low fluorescence intensity.

At the sight of the results obtained, it can be concluded that the chosen distribution of concentrations, which includes the pure analytes, binary and ternary mixtures, has provided the variability necessary to PARAFAC for modelling adequately the analyte signals; even though the spectra were highly overlapped and the number of calibration samples was small.

4.2. Analysis of dried lime tree flowers samples.

4.2.1. Quenching effect.

Several additions of the three analytes studied in this work were performed on a lime flowers blank, which was prior extracted with ethyl acetate and reconstituted in methanol. Specifically, there were 3 additions of carbaryl to obtain a concentration of 29 μg L^{-1} in each addition (range from 0 to 87 μg L^{-1}), 4 additions of carbendazim to obtain 50 μg L^{-1} in each addition (range from 0 to 200 μg L^{-1}) and 3 additions of 1-naphthol to obtain 11 μg L^{-1} in each addition (range from 0 to 33 μg L^{-1}). The analytes were added alternately one by one, starting the first addition with carbendazim, next carbaryl and finally 1-naphthol. The EEM spectra of the lime flowers extract (blank) and of each addition were registered. The ten additions provided the same EEM matrix as the lime flowers extract, both in form and in fluorescence intensity, as it is shown in Fig. 4 (a) and (b) for the extract and the last addition, respectively. This indicates the existence of quenching effect due to the matrix.

A data tensor $\mathbf{X_1}$ (38 × 206 × 11), which contained the 27 samples of the calibration performed in methanol (tensor **X** of section 4.1), the lime flowers extract and the ten additions, was built. In the new PARAFAC decomposition carried out with the data tensor $\mathbf{X_1}$, five factors were necessary, with explained variance of 99.90% and CORCONDIA equal to 83% and no outlier data were found once Q and T^2 statistics were applied. Four of these factors were the same as those obtained in the calibration in methanol (section 4.1), which correspond to the analytes and the background; whereas the other factor is the fluorescence of the matrix (see Fig. 4 (c)). In fact, the correlation between this last factor and the pure lime flowers extract spectra is 0.978 for emission and 0.997 for excitation. In the sample mode (Fig. 4 (d)), the loadings linked to the matrix for the first 27 samples of the calibration in methanol are null; whereas those corresponding to the factors linked to the analytes follow the expected pattern. The problem lies in the factors linked to the analytes in the lime flowers samples (samples 28 to 38) because they have null values, whereas the loadings of the factor corresponding to the matrix are high and constant. This means that all the

fluorescence in these samples is attributable to the matrix as a result of the quenching effect. Thus, the PARAFAC decomposition describes the experimental data and it cannot show the intermediate processes of the quenching with the fluorophores due to there is not any change in the overall fluorescence as a result of the quenching effect. Furthermore, this effect is non linear and PARAFAC is not suitable to fit it.

4.2.2. Analysis of fluorescent signals in different dilutions of the lime flowers extract.

Nine dilutions of the lime flowers extract were prepared in methanol, specifically: 4.5 mL; 4 ml; 3.5 mL; 3 mL; 2.5 mL; 2 mL; 1.5 mL; 1 mL and 0.5 mL of the dried lime tree flowers extract were added to 5 mL volumetric flasks completing to the mark. The EEM matrices recorded of the undiluted lime flowers extract (Fig. 4 (a)) and of the different dilutions of that extract (see Fig. 5) show that there are important changes in fluorescence with the dilution. There are two emission maxima: at 344 nm and 450 nm. From the second dilution (4 mL of the lime flowers extract, Fig. 5 (b)), the fluorescence intensity of the emission region whose maximum is at 344 nm begins to increase and continues increasing up to the eighth dilution (1 mL of the lime flowers extract, Fig. 5 (h)). On the other hand, the fluorescence intensity in the emission region with maximum at 450 nm increases up to the fifth dilution (2.5 mL of the lime flowers extract, Fig. 5 (e)) and, from that point, it decreases to be almost negligible in the last dilution (0.5 mL of the lime flowers extract, Fig. 5 (i)).

On the last dilution, five additions of the analytes were performed in such a way that the concentrations were: i) 100 μg L^{-1} of carbendazim; ii) 100 μg L^{-1} of carbendazim and 57 μg L^{-1} of carbaryl; iii) 100 μg L^{-1} of carbendazim, 57 μg L^{-1} of carbaryl and 23 μg L^{-1} of 1-naphthol; iv) 100 μg L^{-1} of carbendazim, 86 μg L^{-1} of carbaryl and 23 μg L^{-1} of 1-naphthol; and v) 100 μg L^{-1} of carbendazim, 86 μg L^{-1} of carbaryl and 35 μg L^{-1} of 1-naphthol. In this case, a change in fluorescence intensity appears in each of the previous additions; in fact, the variation in the fluorescent intensity from the first to the fifth addition is 200. This behaviour is different from the one observed in the experience of section 4.2.1 and shows that the quenching effect is reduced enough so the fluorescence of the three analytes can be observable and; thus,

these analytes can be quantified using a calibration model based on PARAFAC decomposition.

Taking into account that the two last dilutions (eighth and ninth) had a similar appearance (see Fig. 5), a data tensor $\mathbf{X_2}$ was built arranging the tensor **X** of section 4.1 (Calibration in methanol) with the EEM matrices of the last two dilutions of the lime flowers extract and the ones corresponding to the five additions carried out on the last dilution.

Since carbaryl, carbendazim and 1-naphthol are present in the calibration samples; there would be three factors at least. The three-factor PARAFAC model obtained from the data tensor $\mathbf{X_2}$ had a CORCONDIA of 83% but this model was not coherent (with the true profiles) in any of the three modes. Then, the PARAFAC model with four factors was considered (CORCONDIA: 65%) but the loadings of the sample mode for carbendazim were not coherent. The same happened when the five-factor PARAFAC model was taken into account (CORCONDIA < 0). So, it is observed that a high CORCONDIA value does not imply that the loadings of the model are consistent with the experimental knowledge. If there is no coherence, the model is not valid. However, the loadings of the six-factor PARAFAC model were coherent with the composition of each sample despite the CORCONDIA was less than zero; that is, despite the tensor was not trilinear. Three of the factors of this last model corresponded to the three analytes and the rest corresponded to three fluorophores present in the lime flowers extract.

When the EEM matrix of the sample corresponding to the dilution that precedes those already included was added to the tensor $\mathbf{X_2}$, the results were not coherent with the composition of the samples. Therefore, the lime flowers extract 5 times diluted is the most adequate dilution to carry out the determination of the analytes because the effect is sufficiently reduced to recover the fluorescence spectra.

4.2.3. Quantification and identification of the analytes in the dried lime tree flowers matrix.

The experimental strategy followed in this work to achieve the quantitative determination of ternary mixtures of the three analytes in the lime flowers matrix was to prepare a calibration,

using the standard addition method, based on a D-optimal design (to select a suitable distribution of concentrations) and using the adequate dilution of the lime flowers extract chosen in section 4.2.2 to minimize the quenching effect. Each analyte was at five levels of concentration, being 100 μg L^{-1} the central level for carbaryl and carbendazim. The added concentrations were: 0, 50, 100, 150 and 200 μg L^{-1} of carbaryl and carbendazim, and 0, 10, 20, 30 and 40 μg L^{-1} for 1-naphthol. Therefore, the number of candidate experiments necessary for the initial factorial design would be: $N_c = 5^3 = 125$ experiences. To reduce the experimental effort to an acceptable level, it was proposed to select 25 standards among the 125 through a D-optimal design, with 5 pure standards of increasing concentrations for each analyte as protected points of the design; that is, 13 samples and the 12 remaining samples selected were ternary mixtures. Besides, three replicates of the test sample and five spiked matrix-matched samples were also measured for validation. Table S2 of the "Electronic Supplementary Material" shows the concentrations of the 33 samples of this calibration. The absence of experimental drift was checked through the measure of three methanol blanks throughout the experimentation.

The EEM matrices obtained for each of the samples of the preceding calibration were placed in the order of Table S2 to form the data tensor $\mathbf{X_3}$ of dimensions 33 × 206 × 11. A PARAFAC model was built with the non-negativity constraint imposed for the three ways. Six factors were necessary in the PARAFAC decomposition. Three of the factors corresponded to the three analytes and the rest of the factors were due to fluorophores present in the diluted matrix. The model had a value of explained variance of 99.99%. Despite the loadings were coherent with the composition of each sample; the CORCONDIA was less than zero. The core consistency plot, graph (a) of Figure S1 (Electronic Supplementary Material), shows that there is a lot of no null values of PARAFAC core. This means that the trilinear model was not appropriate. The quantity of each fluorophore of the lime flowers was the same in all the samples due to the standard addition method. Therefore, as explained in the theory section, the data tensor is not trilinear. Taking into account that the amounts of the analytes vary in the measured samples, the CORCONDIA index should increase when the

rest of the components that remain nearly constant are removed from the tensor. The “ad hoc” procedure followed to recover the trilinearity was based on taking away the contribution of the three factors associated with the fluorophores of the lime flowers from the original data tensor $\mathbf{X_3}$.

The procedure used to recover the trilinearity was as follows:

(i) For each one of the three fluorophores of the lime flowers (each of them associated with a factor of the PARAFAC model that will be named as m, n and p), the corresponding excitation-emission matrix was built through the tensor product of the spectral loadings of each factor that are contained in the PARAFAC model. These matrices are normalized, as can be seen in Fig. 6, because the second and third modes in PARAFAC are normalized.

(ii) To obtain the matrix of dimension (206 × 11) in real units of fluorescent intensity, each matrix was multiplied by the sample loading of this factor in each of the measured samples. Thus, a matrix was obtained for each of the samples and for each of the fluorophores.

(iii) Once the preceding matrices were obtained, they were concatenated to form the data tensor $\mathbf{X_i}$ for the i-th fluorophore (i=m,n,p).

(iv) These three tensors were added up $\mathbf{X_F} = \mathbf{X}_m + \mathbf{X_n} + \mathbf{X_p}$ to generate the tensor, $\mathbf{X_F}$, associated with the fluorescence of the lime flowers.

(v) The contribution of the lime flowers was taken away from the original data tensor to obtain the tensor $\mathbf{X_4} = \mathbf{X_3} - \mathbf{X_F}$ associated with the analytes.

(vi) The PARAFAC decomposition was applied to this resultant tensor.

Three factors were necessary, associated with the three analytes, in the PARAFAC decomposition of the new tensor $\mathbf{X_4}$. This model has a CORCONDIA index equal to 100%. No outlier data were found in the models of the tensors $\mathbf{X_3}$ and $\mathbf{X_4}$. The loadings obtained for the three modes were nearly the same in both models, as can be seen in Fig. 7.

The three analytes were unequivocally identified, since their spectral profiles, shown in Fig. 7 (e) for emission and in Fig. 7 (f) for excitation, correspond to the reference spectra. The

correlation coefficients between the emission and excitation spectra and the PARAFAC profiles were equal to 0.986 and 0.994 for carbaryl; 0.980 and 0.974 for carbendazim, and 0.985 and 0.869 for 1-naphthol, respectively.

The calibration curves for each analyte were computed by the regression of the sample loadings *versus* added concentration. The three replicates of the test sample and the five spiked samples were used as test set, whereas the rest of the samples constituted the calibration set (25 in total). Table 2 shows the results of the least squares (LS) regressions obtained with the PARAFAC model of the data tensor $\mathbf{X}_4$. These regressions were significant in all cases and did not have any outlier data. Owing to the use of the standard addition method, the concentration of the diluted lime flowers sample was obtained as usual from the regression loading *versus* added analyte. The results were 33.34, 300.67 and 6.09 μg L^{-1} for carbaryl, carbendazim and 1-naphthol, respectively.

The accuracy lines “calculated concentration *versus* added concentration” were also performed. The slopes and intercepts of these regressions for each case were significantly equal to 1 and 0, respectively. Therefore, the method has not proportional or constant bias.

The decision limit and the capability of detection for each analyte were determined for probabilities of false positive (α) and false negative (β) equal to 0.05, so the values achieved were 3.38 and 6.68 μg L^{-1} for 1-naphthol, 12.5 and 24.75 μg L^{-1} for carbaryl, and 37.58 and 74.37 μg L^{-1} for carbendazim, respectively, as Table 2 shows. As for the calibration in pure solvent (Section 4.1, Table 1), the highest values were obtained for carbendazim as a result of its low sensitivity. For the three analytes, both CCα and CCβ were higher than those obtained in methanol; mainly due to a residual standard deviation higher for the accuracy line obtained with matrix-matched standards (Table 2) than for the accuracy line obtained with standards in solvent (Table 1).

The lowest values of the mean absolute values of the relative errors were obtained for carbaryl: 5.84% (n=16) in calibration and 4.02% (n=5) in prediction. For carbendazim, these values were higher: 20.85% (n=16) and 38.67% (n=5), respectively. However, when the

samples with concentration lower than CCβ are not considered, the mean of the absolute values of the relative errors decreases to 10.42% (n=11) and 11.80% (n=2) respectively, as Table 2 shows. These mean values in prediction are similar to those obtained when the samples were prepared in pure solvent (Table 1).

The MRL for carbaryl and carbendazim is 100 μg Kg^{-1} in lime flowers, so it is necessary to calculate for both analytes the decision limit and the capability of detection for x_0 = 100 μg L^{-1}. In this context, the probabilities α and β are called false non-compliance and false compliance, respectively. For substances with a MRL established, the capability of detection at the MRL is defined for a given probability of false non-compliance, α, as the true net concentration of the analyte in the material to be analyzed which will lead, with probability $1-\beta$, to the correct conclusion that the concentration in the analyzed material is greater than MRL. The values of decision limit, CCα (for a probability of false non-compliance equal to 0.05) and the capability of detection, CCβ (for probabilities of false non-compliance and false compliance equal to 0.05) estimated at the MRL of 100 μg L^{-1} were 112.3 and 124.3 μg L^{-1} for carbaryl, respectively, and 136.8 and 172.9 μg L^{-1} for carbendazim, respectively.

The difficulty in the quantification of the carbamates in lime flowers is clearly shown in Fig. 8. This is mainly due to the high overlapping between the analytes and the matrix, the small variation in the fluorescent intensity when the analytes are added to that matrix and the similarity between the obtained spectra. The estimation of the capability of detection of the PARAFAC calibration for each of the analytes depends on the sensibility (slope of the calibration) and its standard deviation [**Error! Bookmark not defined.**]. Thus, its analysis enables to explore the limit of the quantitative possibilities of the calibration with EEM signals through PARAFAC. In general, some kind of change in the quantitative characteristics will appear when the concentration range is reduced (the magnitude of the signal is also reduced). For this analysis, the concentrations of the samples were reduced by 50% for carbaryl, by 30% for carbendazim and by 40% for 1-naphthol with regard to Table S2. Therefore, the levels of concentration in this case were: 0, 25, 50, 75 and 100 μg L^{-1} for

carbaryl, 0, 35, 70, 105 and 140 μg L^{-1} for carbendazim, whereas for 1-naphthol they were 0, 6, 12, 18 and 24 μg L^{-1}. A PARAFAC model of six factors was chosen, due to the coherence in the visual appearance of the loadings, for the data tensor $\mathbf{X_5}$ (33 × 206 × 11), which was formed by the EEMs of this last calibration. As in the previous case (data tensor $\mathbf{X_4}$), three of the factors corresponded to the analytes and the rest of the factors were due to fluorophores of the lime flowers. This model had a value of explained variance of 99.99%, a CORCONDIA less than zero and there were not outliers. The core consistency plot, graph (b) of Figure S1 (Electronic Supplementary Material), shows that there is a lot of no null values of PARAFAC core. Following the strategy described above of subtracting the fluorescence attributable to lime flowers, a PARAFAC model of three factors was obtained with a CORCONDIA index equal to 99%.

The three analytes were unequivocally identified by the correlation between the pure spectra and the PARAFAC spectral loadings. In all cases, the correlation coefficients were greater than 0.97 for the emission and excitation profiles, except for the correlation for the excitation for 1-naphthol and carbendazim. While in this new analysis there is some improvement in this value for the former analyte because the value rises from 0.87 to 0.92; it gets worse for the latter (the value decreases from 0.97 to 0.73). In this sense, it must be noticed that only two concentrations of the calibration for carbendazim are above the capability of detection, CCβ, obtained. This makes difficult the recovery of its excitation spectrum; however, the emission spectrum is not affected.

Two different calibration curves “sample loadings *versus* added concentration” were performed for each analyte. In the first case, all the samples were used as calibration set (25 mixture samples) except for the three replicates of the test sample and the five spiked samples which formed the test set. The second case was based on performing those regressions considering only the samples that contain one of the analytes (5 samples, including the zero value) and the rest of the samples were used as the test set (28 samples). The results for both cases and for each analyte are shown in Table 3 together with some validation parameters. In all cases, the regressions were significant. One outlier was

detected and eliminated from the calibration set for 1-naphthol and another one for carbendazim, the latter in the regression performed with pure samples; because both had standardized residual greater than 2.5.

For each analyte, the slope and intercept of both regressions are very similar. On the other hand, the residual standard deviation is similar or lower in the regression in which only samples that contain a single analyte are considered. This is reasonable because in the calibration performed with binary and ternary mixtures there is more variability in the signals, not related to the variation in the concentration of the calibrated analyte.

The concentration in the lime flowers sample as well as its confidence interval at 5% of significance level for the determination with the spiked samples that only contain a calibrated analyte have also been listed in Table 3. It must be noticed that the concentrations determined with all the samples are within these confidence intervals, so the presence of other analytes in the calibration samples does not introduce any bias in the determinations.

To verify the trueness of the method, it has been evaluated if the intercept (b_0) and the slope (b_1) of the accuracy line were significantly equal to 0 and 1, respectively. It can be concluded that the method is accurate for all the analytes at 95% confidence level because the p-values of the corresponding tests were always greater than 0.05.

When the decision limit and the capability of detection of the four calibrations collected in Tables 1, 2 and 3 are compared, it is concluded that the results are slightly worse in lime flowers than in methanol. The effect of calibrating with binary and ternary samples of the analytes highly depends on the ratio between the residual standard deviation (not explained by the amount of analyte) and the slope of the regression. This effect is collected in the residual standard deviation of the accuracy line [49] so the decision limit for carbaryl and 1-naphthol improves and reaches the values obtained in methanol. However, this does not happen for carbendazim, whose decision limit gets worse because the value rises from 37.6 to 51.7 $\mu g\ L^{-1}$ when the calibration range is reduced. This result is coherent with the low signal-to-noise ratio for this analyte which is related to the poor recovery of its excitation spectrum. The analysis for the capability of detection is similar.

The amount of carbaryl, carbendazim and 1-naphthol found in the lime flowers samples is very high, particularly in the second sample. To evaluate this, it must bear in mind that carbaryl and especially carbendazim are very persistent and that carbendazim is used to treat the diseases of lime trees. Similar amounts of carbendazim, even higher than those found in the first sample, have been found in other agricultural products such as broccoli and celery leaves [**Error! Bookmark not defined.**].

The determination of carbamates in dried lime tree flowers presents some difficulties with regard to their determination in methanol, as it is clearly shown when figures 8 and 3 are compared. These difficulties are caused by the low fluorescence intensity of carbendazim together with the signals more overlapped than in methanol because the lime flowers contains fluorophores that emit in the same region as the analytes. The presence of the other carbamates introduces a high residual variability as it is shown in the regression performed with all the samples in Table 3.

5. Conclusions

The proposed methodology, based on PARAFAC decomposition of EEM matrices, allows to identify and quantify two carbamate pesticides (carbaryl and carbendazim) and the degradation product of carbaryl (1-naphthol) in dried lime tree flowers, through an experimental strategy that minimize the quenching effect despite the presence of other fluorophores that emit fluorescence in the same region as the analytes.

In spite of the difficulty (small magnitude of the fluorescent signal and the highly overlapped spectra between the matrix and the analytes), the identification has been possible and the influence on the capability of detection has been assessed. Furthermore, the figures of merit have been evaluated in solvent and in matrix-matched solutions (dried lime tree flowers).

6. Acknowledgements

The authors thank the financial support provided by projects of the Ministerio de Economía y Competitividad (CTQ2011-26022) and Junta de Castilla y León (BU108A11-2). L. Rubio is particularly grateful to Universidad de Burgos for her FPI grant.

References

[1] M.V. Bosco, M. Garrido, M.S. Larrechi, Anal. Chim. Acta 559 (2006) 240–247.

[2] C.M. Andersen, R.Bro, J. Chemom. 17 (2003) 200-215.

[3] F. Alarcón, M.E. Báez, M. Bravo, P. Richter, G.M. Escandar, A.C. Olivieri, E. Fuentes, Talanta 103 (2013) 361–370.

[4] X.D. Qing, H.L. Wun, C.C. Nie, X.F. Yan, Y.N. Li, J.Y. Wang, R.Q. Yu, Talanta 103 (2013) 86–94.

[5] Y.N. Li, H.L. Wu, X.D. Qing, C.C. Nie, S.F. Li, Y.J. Yu, S.R. Zhang, R.Q. Yu, Talanta 85 (2011) 325–332.

[6] Y. Ni, Q. Zhang, S. Kokot, Analyst 135 (2010) 2059–2068.

[7] F. Cañada-Cañada, A. Espinosa-Mansilla, A. Muñoz de la Peña, A. Jiménez Girón, D. González-Gómez, Food Chem. 113 (2009) 1260–1265.

[8] R. Morales, M.C. Ortiz, L.A. Sarabia, M.S. Sánchez, Anal. Chim. Acta 707 (2011) 38-46.

[9] M.C. Ortiz, L.A. Sarabia, M.S. Sánchez, D. Giménez, Anal. Chim. Acta 642 (2009) 193–205.

[10] A. Muñoz de la Peña, N. Mora Díez, D. Bohoyo Gil, A.C. Olivieri, G.M. Escandar, Anal. Chim. Acta 569 (2006) 250–259.

[11] M.C. Hurtado-Sánchez, I. Durán-Merás, M.I. Rodríguez-Cáceres, A. Jiménez-Girón, A.C. Olivieri, Talanta 88 (2012) 609–616.

[12] J. Nie, H. Wu, X. Wang, Y. Zhang, S. Zhu, R. Yu, Anal. Chim. Acta 628 (2008) 24–32.

[13] C. D. Bernardes, R.J. Poppi, M.M. Sena, Talanta 82 (2010) 640–645.

[14] S. Leurgans, R.T. Ross, Stat. Sci. 7 (1992) 289-319.

[15] N. Rodríguez, M.C. Ortiz, L.A. Sarabia, Talanta 77 (2009) 1129-1136

[16] R.D. JiJi, G.A. Cooper, K.S. Booksh, Anal. Chim. Acta 397 (1999) 61–72.

[17] C. K. Winter, Pesticides and Herbicides: Toxicology, Encyclopedia of Food Science and Nutrition, second ed., Elsevier Science Ltd., 2003, pp. 4494-4501.

[18] Handbook of Pesticides, Methods of Pesticide Residues Analysis. Edited by Leo M.L. Nollet, Hamir Singh Rathore, CRC Press, Taylor & Francis Group, 2010.

[19] M. Asensio-Ramos, J. Hernández-Borges, T. M. Borges-Miquel, M.A. Rodríguez-Delgado, J. Chromatogr. A 1218 (2011) 4808– 4816.

[20] S. Wang, H. Mu, Y. Bai, Y. Zhang, H. Liu, J. Chromatogr. B 877 (2009) 2961–2966.

[21] N. Rosales-Conrado, M.E. León-González, L.V. Pérez-Arribas, L.M. Polo-Díez, J. Chromatogr. A 1081 (2005) 114–121.

[22] M. Liu, Y. Hashi, Y. Song, J.M. Lin, J. Chromatogr. A 1097 (2005) 183–187.

[23] S.W.C. Chung, B.T.P. Chan, J. Chromatogr. A 1217 (2010) 4815–4824.

[24] A. Mostafa, G. Medley, D.M. Roberts, M. Sayed Mohamed, A.A. Elshanawanif, M.S. Roberts, X. Liu, J. Chromatogr. B 879 (2011) 2234– 2238.

[25] R. Carabias-Martínez, C. García-Hermida, E. Rodríguez-Gonzalo, L. Ruano-Miguel, J. Sep. Sci. 28 (2005) 2130–2138.

[26] S.H. Zhu, H.L. Wu, A.L. Xia, Q.J. Han, Y. Zhang, R.Q. Yu, Talanta 74 (2008) 1579–1585.

[27] R.M. Maggio, P.C. Damiani, A.C. Olivieri, Anal. Chim. Acta 677 (2010) 97–107.

[28] S.H. Zhu, H.L. Wu, A.L. Xia, J.F. Nie, Y.C. Bian, C.B. Cai, R.Q. Yu, Talanta 77 (2009) 1640–1646.

[29] Commission REGULATION (EC) No 149/2008 of 29 January 2008. Off J L58:1–398.

[30] COMMISSION REGULATION (EU) No 559/2011 of 7 June 2011. Off J L152:1–21.

[31] COMMISSION REGULATION (EU) No 899/2012 of 21 September 2012. Off J L273:1–75.

[32] Rapid Alert System for Food and Feed, RASFF Portal, DG Sanco, Bruxelles https://webgate.ec.europa.eu/rasff-window/portal/index.cfm (Accessed 11/11/2013).

[33] International programme on chemical safety. Joint with WHO/FAO Expert Committee on Food Additives http://www.inchem.org (Accessed 11/11/2013)

[34] D. Mathieu, J. Nony, R. Phan-Tan-Luu, NemrodW (Versión 2007_03), L.P.R.A.I. Marseille, France, 2007.

[35] C.A. Andersson, INCA 1.41, Department of Food Science, University of Copenhagen, Denmark. Available at http://www.models.life.ku.dk/inca (Accessed 11/11/2013).

[36] B. M. Wise, N.B. Gallagher, R. Bro, J.M. Shaver, W. Winding, R.S. Koch, PLS Toolbox 6.0.1, Eigenvector Research Inc., Manson, WA.

[37] STATGRAPHICS Centurion XVI Versión 16.1.05 (32 bit). Statpoint Technologies, Inc. 2010.

[38] L .A. Sarabia, M.C. Ortiz, Trends Anal. Chem. 13 (1994) 1-6.

[39] R. Bro, Chemom. Intell. Lab Syst. 46 (1999) 133-147.

[40] C.A. Anderson, R. Bro, Chemom. Intell. Lab. Syst. 52 (2000) 1-4.

[41] R. B. Cattell, Psychometrika 9 (1944) 267-283.

[42] K. S. Booksh, B. R. Kowalski, *Anal. Chem.* 66 (1994) 782A–791A.

[43] R. Bro, H.A.L Kiers, J. Chemom. 17 (2003) 274–286.

[44] R. Bro Multi-way Analysis in the food Industry.Models Algorithms and applications. Doctoral Thesis, University of Amsterdam, Amsterdam The Netherlands 1998 (http://www.models.kvl.dk/sites/default/files/brothesis_0.pdf. (Accessed January 2014)

[45] International Organization for Standardization, ISO 11843, Capability of detection. Part 1: Terms and definitions, 1997; and Part 2: Methodology in the linear calibration case, 2000. Geneva, Switzerland.

[46] J. Inczédy, T. Lengyel, A.M. Ure, A. Gelencsér, A. Hulanicki, Compendium of Analytical Nomenclature IUPAC, 3rd ed., Pot City Press Inc., Baltimore, 2000.

[47] 2002/657/EC Commission Decision of 12 August 2002, Brussels, Off. J. Eur. Commun. L221 (August) (2002) 8-36.

[48] M.C. Ortiz, L.A. Sarabia, I. García, D. Giménez, E. Meléndez, Anal. Chim. Acta 559 (2006) 124–136.

[49] M.C. Ortiz, L.A. Sarabia, M.S. Sánchez, Anal. Chim. Acta 674 (2010) 123-142.

Table 1 Results of the regression of sample loading *versus* true concentration (C_{true}) and of the accuracy line of calculated concentration (C_{calc}) *versus* C_{true} for carbaryl, carbendazim and 1-naphthol (Calibration in methanol, Section 4.1).

	Carbaryl	Carbendazim	1 – naphthol
Regression of sample loading vs. C_{true}			
Slope, b_1	47.817	6.878	123.938
Intercept, b_0	- 47.141	348.99	37.827
Residual standard deviation, s_{yx}	97.564	87.050	201.035
Correlation coefficient, ρ	0.998	0.981	0.992
Number of outliers removed	-	1 (sample 8)	-
$\overline{\lvert e_r \rvert}_{\text{calibration}}$ [a]	4.13 (n=15)	10.07 (n=14)	8.38 (n=15)
$\overline{\lvert e_r \rvert}_{\text{prediction}}$ [a]	3.48 (n=5)	10.90 (n=6)	6.80 (n=5)
Regression of C_{calc} vs. C_{true}			
Slope, b_1	1	1	0.999
Intercept, b_0	$7.651 \cdot 10^{-7}$	$-2.511 \cdot 10^{-6}$	$2.363 \cdot 10^{-7}$
Residual standard deviation, s_{yx}	2.040	12.656	1.622
Decision limit, CCα (x_0 = 0) (µg L^{-1})	3.74	23.25	2.97
Capability of detection, CCβ (x_0 = 0) [b] (µg L^{-1})	7.38	45.89	5.86

[a] $\overline{\lvert e_r \rvert}$ is the mean absolute value of the relative error.

[b] α = β = 0.05

Table 2 Results of the regression of sample loading *versus* added concentration (C_{added}) and of the accuracy line for carbaryl, carbendazim and 1-naphthol performed with the model of the data tensor ($\mathbf{X}_4$) (standard addition calibration in dried lime tree flowers, Section 4.2.3).

	Carbaryl	Carbendazim	1 – naphthol
Regression of sample loading vs. C_{added}			
Slope, b_1	16.153	1.7031	29.245
Intercept, b_0	538.523	512.076	178.206
Residual standard deviation, s_{yx}	113.11	35.838	55.292
Correlation coefficient, ρ	0.996	0.965	0.993
Number of outliers removed	-	-	-
Sample concentration (µg L^{-1})	33.34	300.67	6.09
$\overline{\lvert e_r \rvert}_{\text{calibration}}$ [a]	5.84 (n=16)	10.42 [b] (n=11)	7.66 (n=16)
$\overline{\lvert e_r \rvert}_{\text{prediction}}$ [a]	4.02 (n=5)	11.80 [b] (n=2)	4.44 (n=5)

Accuracy line			
Slope, b_1	0.999	0.999	1
Intercept, b_0	$- 8.844 \cdot 10^{-6}$	$- 1.912 \cdot 10^{-4}$	$- 9.769 \cdot 10^{-6}$
Residual standard deviation, s_{yx}	7.002	21.043	1.891
Decision limit, CCα ($x_0 = 0$) (μg L^{-1})	12.5	37.58	3.38
Capability of detection, CCβ ($x_0 = 0$) [c] (μg L^{-1})	24.75	74.37	6.68
CCα (x_0 = 100 μg L^{-1})	112.3	136.8	-
CCβ (x_0 = 100 μg L^{-1}) [c]	124.3	172.9	-

[a] $\overline{|e_r|}$ is the mean absolute value of the relative error.

[b] Samples with calculated concentration lower than the capability of detection obtained were excluded.

[c] α = β = 0.05

Table 3 Results of the regression of sample loading *versus* added concentration (C_{added}) and of the regression of calculated concentration (C_{calc}) *versus* C_{added} for carbaryl, carbendazim and 1-naphthol, performed considering mixtures or only pure samples as calibration set, for the second calibration (data tensor $\mathbf{X}_5$) carried out in dried lime tree flowers matrix.

	With mixtures			
	Carbaryl	Carbendazim	1 – naphthol	Carbaryl
Regression of sample loading vs. C_{added}				
Slope, b_1	21.699	2.200	42.337	22.838
Intercept, b_0	1759.29	3602.02	3241.37	1710.82
Residual standard deviation, s_{yx}	52.741	63.745	38.106	66.046
Correlation coefficient, ρ	0.998	0.883	0.996	0.998
Number of outliers removed	-	-	1 (sample 20)	-
Sample concentration (μg L^{-1})	81.08	1637.28	76.56	74.91
Interval for sample concentration (at 95% confidence level)				(58.73,99.53)
$\overline{\|e_r\|}_{calibration}$ [a]	4.02 (n=16)	26.95 [b] (n=4)	5.63 (n=15)	4.61 (n=4)
$\overline{\|e_r\|}_{prediction}$ [a]	12.08 (n=5)	- [b]	6.29 (n=5)	6.02 (n=17)
Regression of C_{calc} vs. C_{added}				
Slope, b_1	0,999	1	1	1

Intercept, b_0	$-6.584 \cdot 10^{-5}$	$1.143 \cdot 10^{-10}$	$-2.468 \cdot 10^{-5}$	$1.4 \cdot 10^{-9}$
Residual standard deviation, s_{yx}	2.431	28.980	0.9001	2.892
Decision limit, CCα (x_0 = 0) (µg L^{-1})	4.34	51.75	1.61	8.61
Capability of detection, CCβ (x_0 = 0) [c] (µg L^{-1})	8.59	102.4	3.18	16.3

[a] $\overline{|e_r|}$ is the mean absolute value of the relative error.

[b] Samples with calculated concentration lower than the capability of detection obtained were excluded.

[c] α = β = 0.05

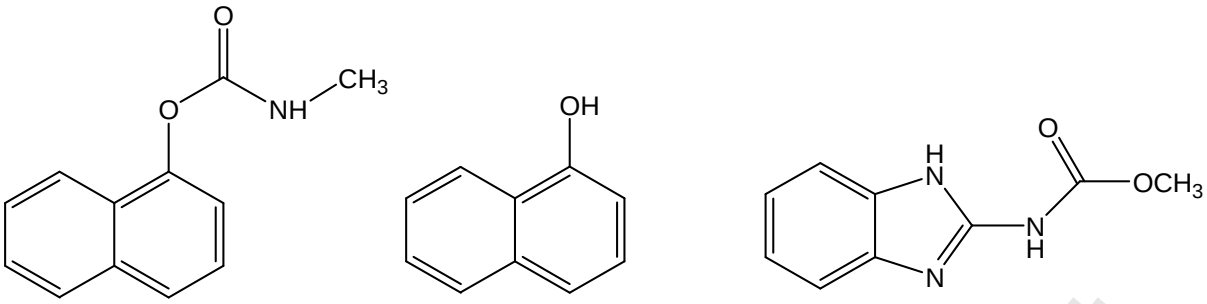

Carbaryl 1 - naphthol Carbendazim

Fig. 1

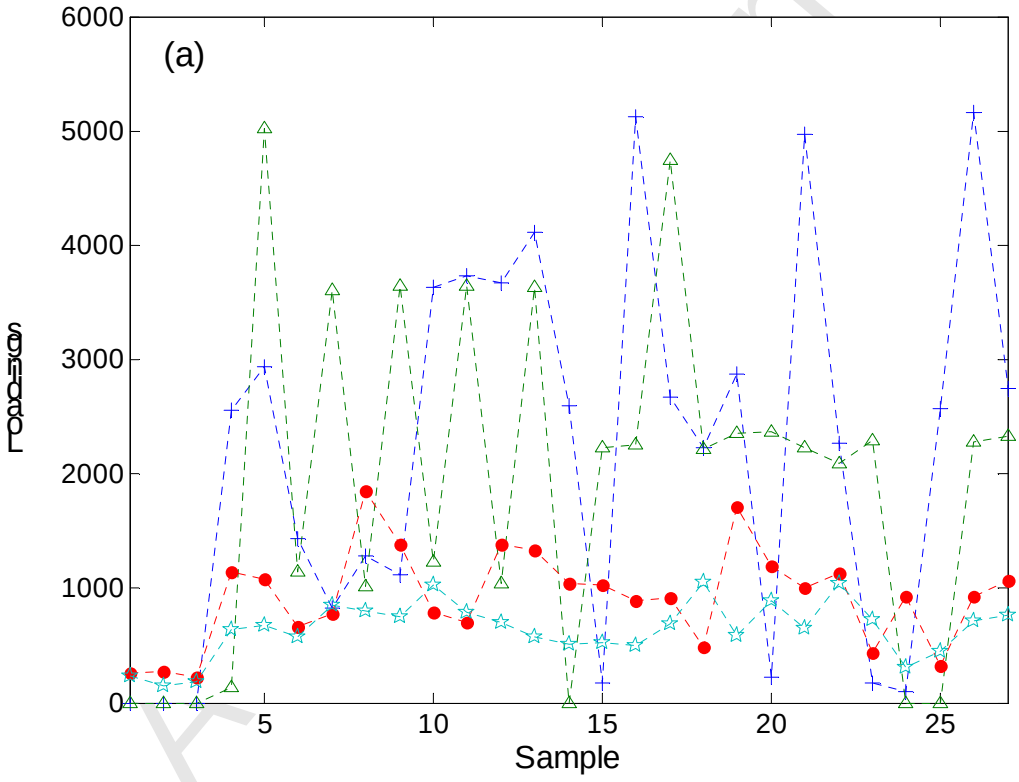

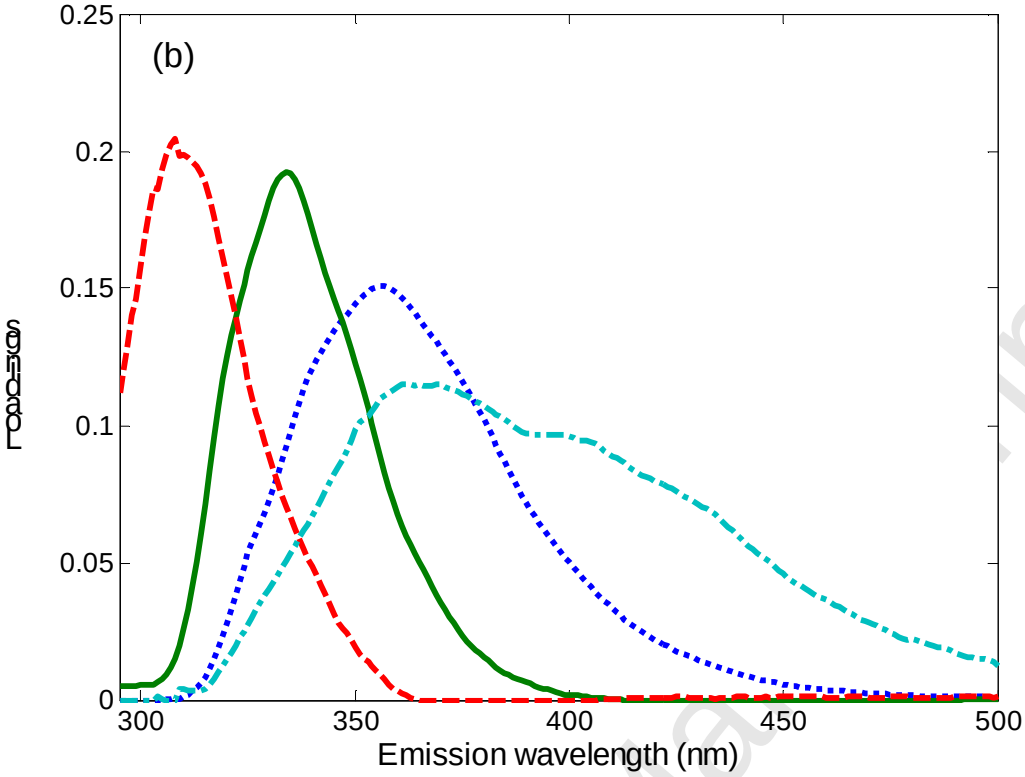

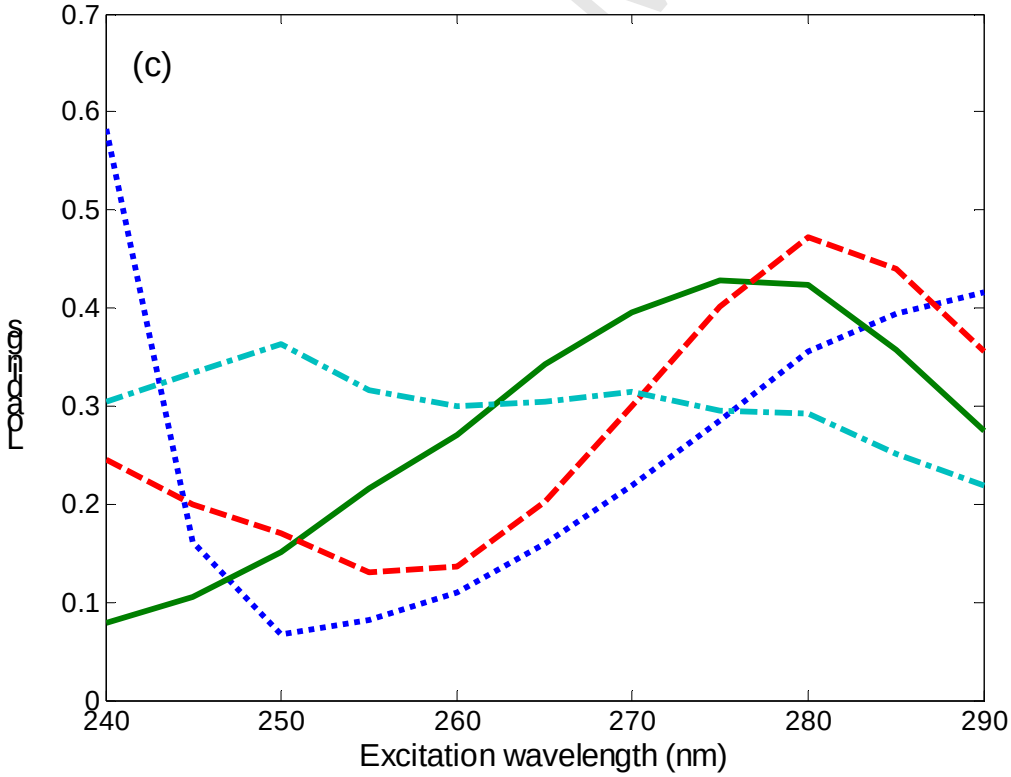

Fig. 2

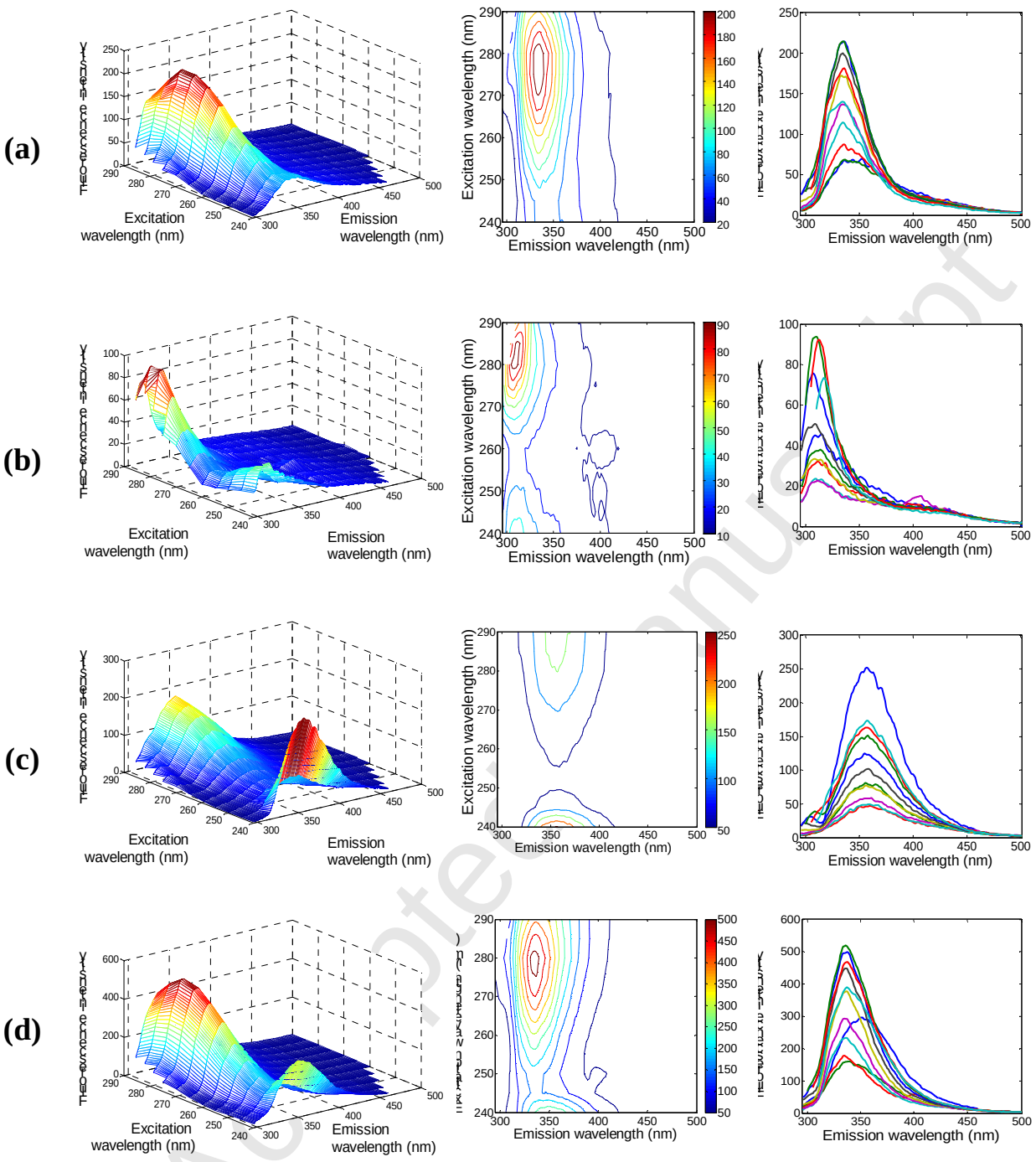

Fig. 3

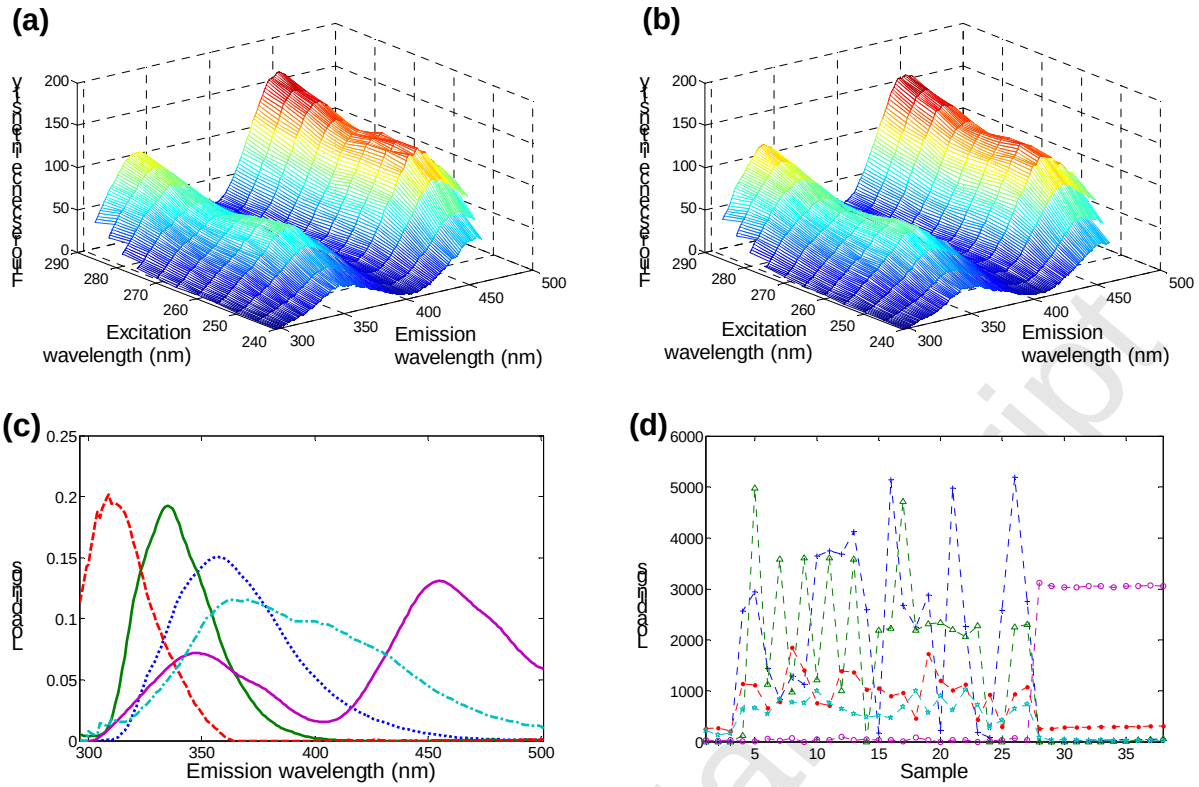

Fig. 4

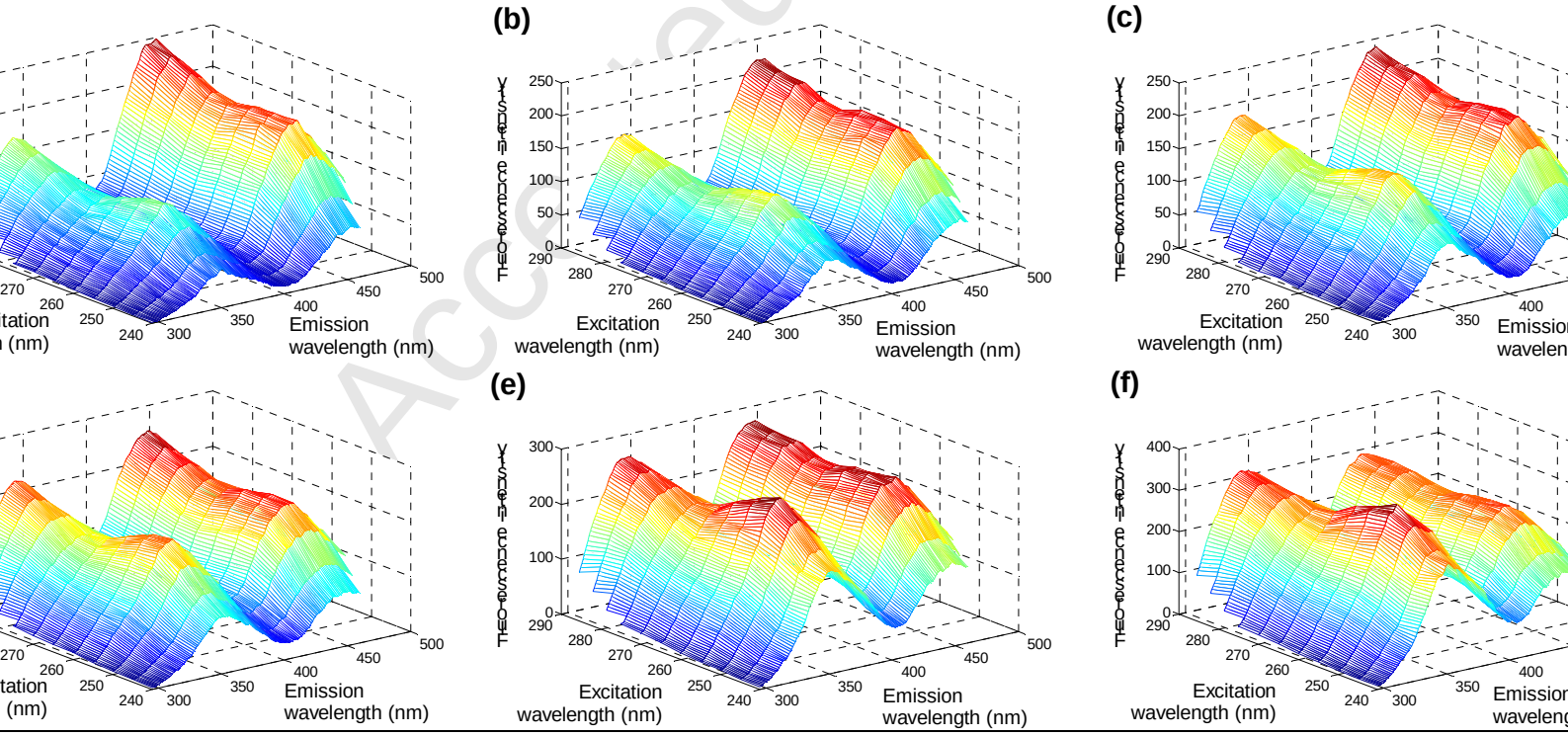

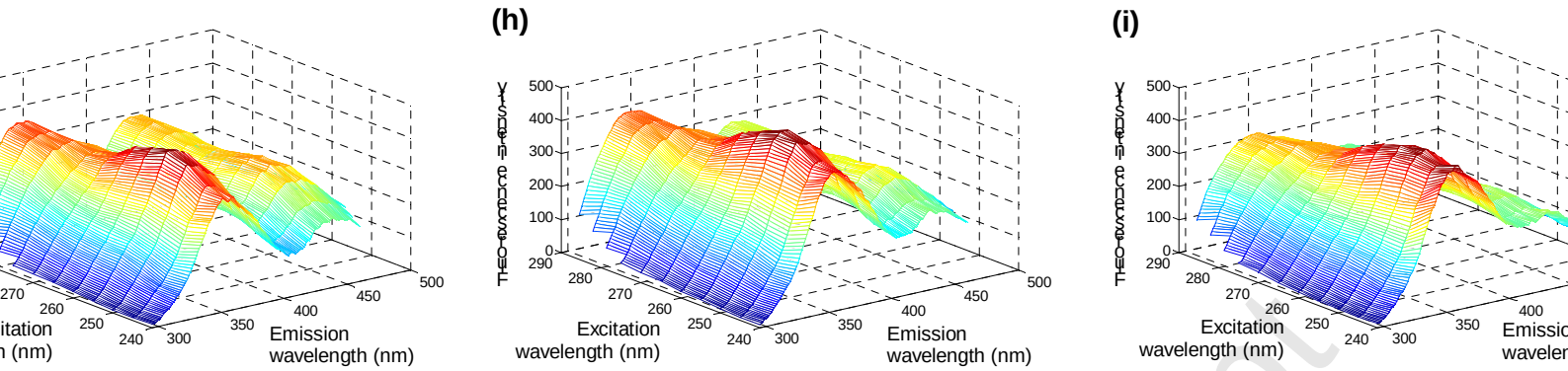

Fig. 5

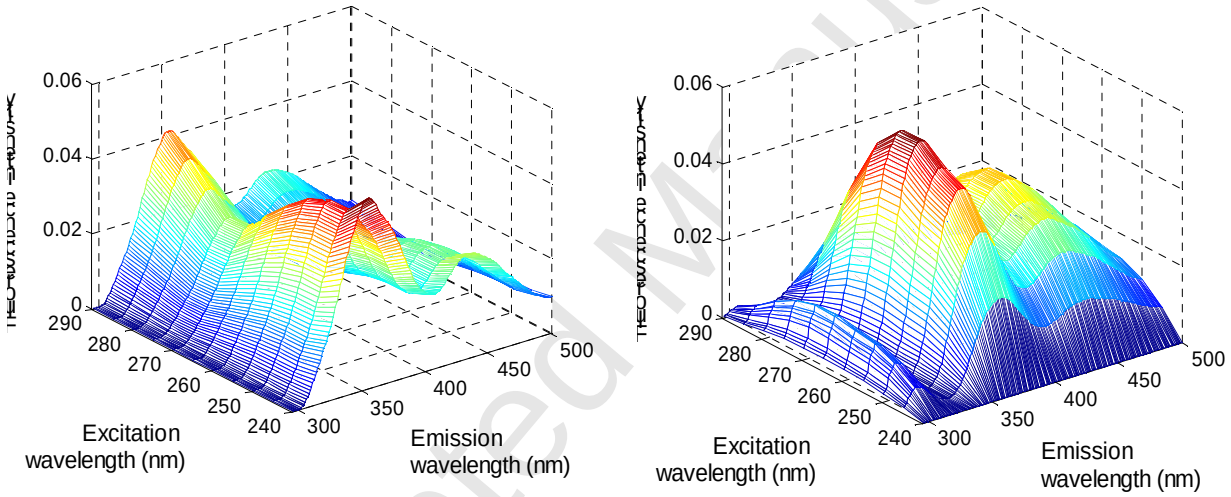

Fig. 6

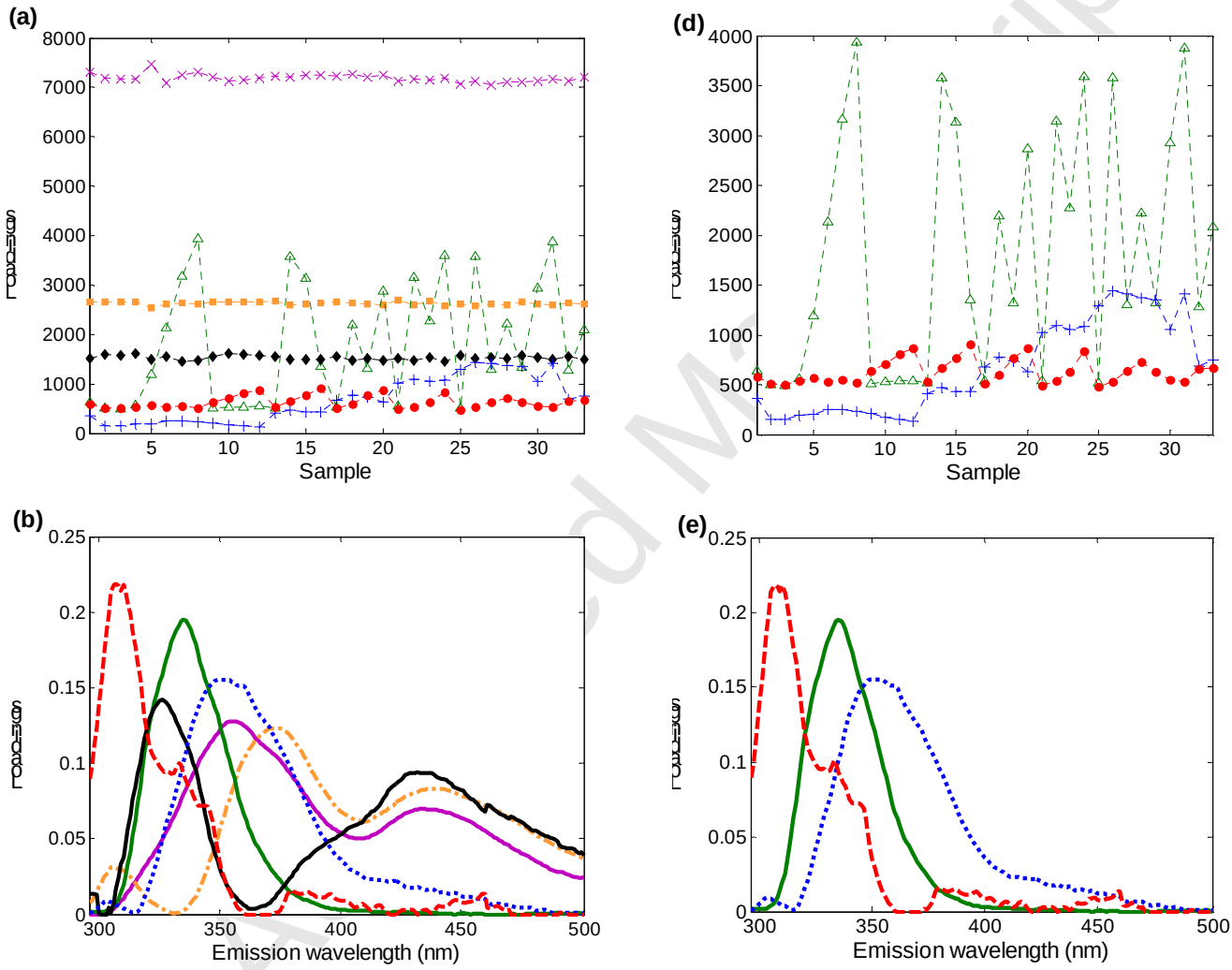

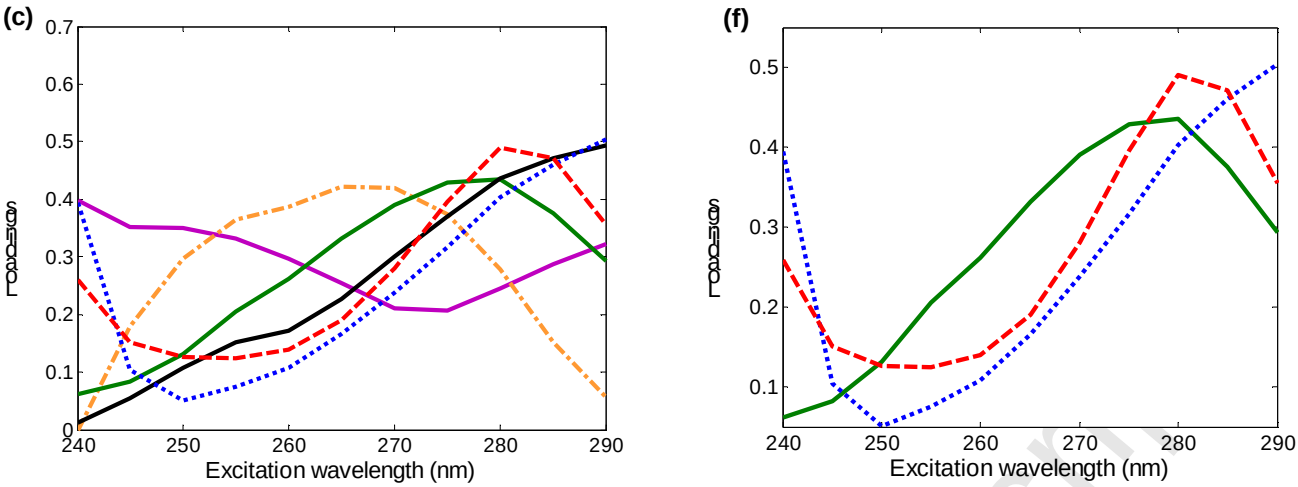

Fig. 7

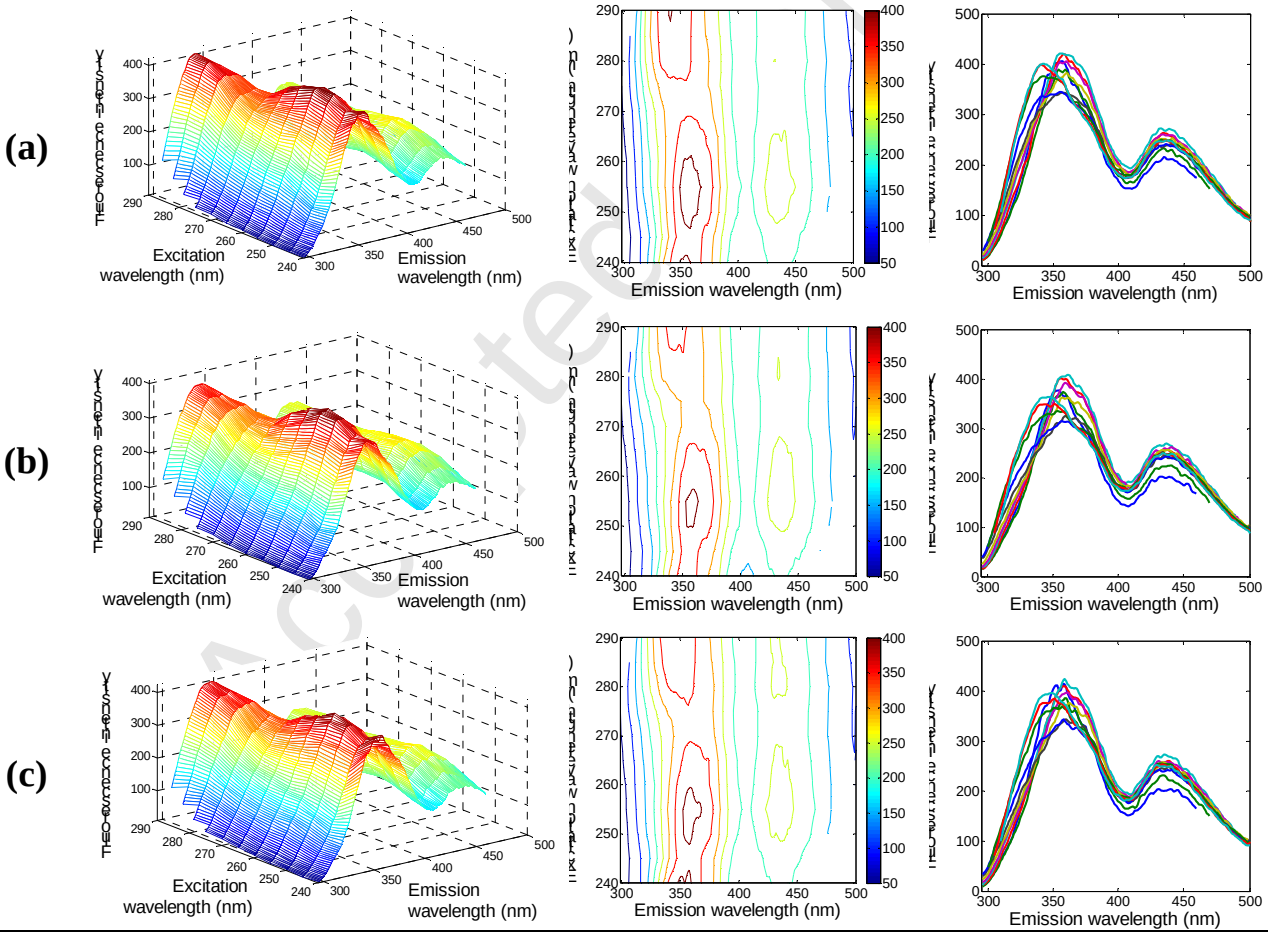

(d)

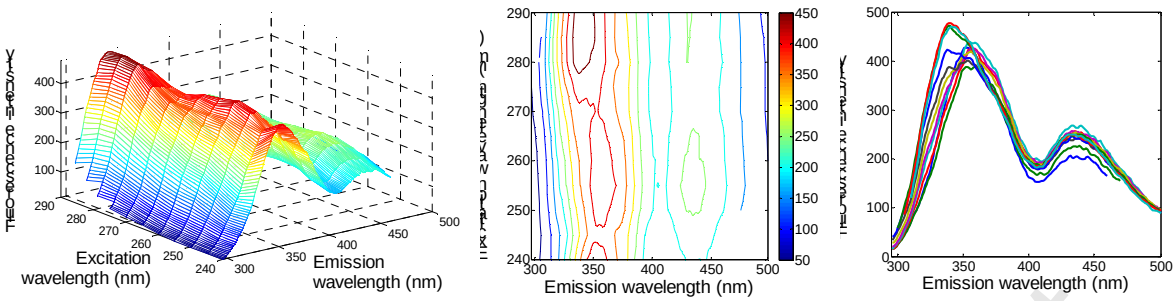

Fig. 8